

# Voltage Scaling and Temperature Effects on Drain Leakage Current Degradation in a Hot Carrier Stressed n-MOSFET

Tahui Wang, C.F. Hsu, L.P. Chiang, N.K. Zous, T.S. Chao\* and C.Y. Chang

Department of Electronics Engineering, National Chiao-Tung University

\*National Nano Devices Lab.,  
Hsin-Chu, Taiwan, R.O.C.

fax:886-3-5724361;email:wang@jekyll.ee.nctu.edu.tw

## ABSTRACT

Drain leakage current degradation at zero  $V_{gs}$  in a hot carrier stressed n-MOSFET is measured and modeled. The dependences of drain leakage current on supply voltage and temperature are characterized. In modeling, various drain leakage current mechanisms including drain-to-source subthreshold leakage current, band-to-band tunneling current and interface trap assisted leakage current are taken into account. Our result shows that interface trap induced leakage current appears to be a dominant drain leakage mechanism as the supply voltage is scaled below 3.0V. Drain leakage current degradation by orders of magnitude has been observed due to hot carrier stress.

## INTRODUCTION

The reduction of drain leakage current at zero  $V_{gs}$  has been a major concern in CMOS device scaling. Gate induced drain leakage (GIDL) current resulting from band-to-band tunneling has been recognized as one of the major drain leakage mechanisms in thin-oxide MOSFET's [1]. Recently, hot carrier stress effects on device degradation have received much interest [2-6]. However, most of the studies concentrate on stress induced on-state drain current reduction [2,3]. The stress effect on off-state drain leakage current degradation has not received as much attention [4,7]. The stress effect on drain leakage current is attributed to the creation of oxide trapped charge and interface traps. The build-up of negative oxide charge shifts the device flat-band voltage and results in an enhancement of band-to-band tunneling current. In addition, the generated interface traps can introduce an additional trap-assisted leakage mechanism [8]. At scaled supply voltages, while band-to-band tunneling can be greatly alleviated, the trap-assisted current may appear to be a dominant leakage mechanism. Furthermore, experimental results showed that the trap-induced leakage current exhibits a dependence on temperature [9]. In a certain bias range, the leakage current becomes much aggravated as temperature rises and thus may have impact on a DRAM refresh time. In this work, it is our intention to investigate the hot carrier stress effect on drain leakage current degradation in thin-oxide MOSFET's. The drain leakage current mechanisms at different supply voltages and temperatures are characterized and modeled.

## DRAIN LEAKAGE CURRENT MECHANISMS

Various drain leakage paths in a stressed MOSFET are considered in our model. The trap-independent leakage mechanisms include band-to-band tunneling current ( $I_{BB}$ ) and drain-to-source subthreshold current ( $I_S$ ),

$$I_{BB} = AE_i^2 \exp(-B/E_i) \quad (1)$$

$$I_S = I_0 \exp\left(\frac{q}{nkT} V_{gs}\right) \quad (2)$$

where the parameters  $A$  and  $B$  are defined in Ref. [10].  $E_i$  denotes the total Si surface field. Drain junction leakage current is small in this work and can be neglected. Fig. 1 illustrates these two components in the lateral direction and in the vertical direction respectively.

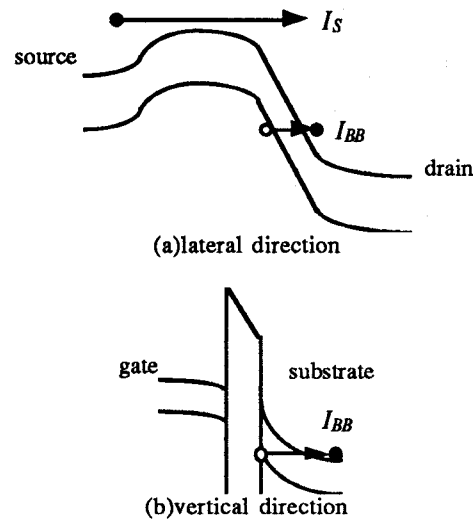


Fig. 1 Illustration of subthreshold leakage current ( $I_S$ ) and band-to-band tunneling current ( $I_{BB}$ ) (a) in the lateral direction and (b) in the vertical direction.

The interface trap assisted leakage mechanisms are the Shockley-Read-Hall current ( $\Delta I_{SRH}$ ), thermionic-field emission current ( $\Delta I_{TF}$ ), and sequential tunneling current ( $\Delta I_{TAT}$ ). A complete trap-assisted drain-to-substrate leakage path at the Si/SiO<sub>2</sub> surface is formed by hole emission from traps to the valence band and electron emission from traps to the conduction band. Both electron emission and hole emission are carried out via either thermionic emission or field emission. The carrier transition processes are drawn in Fig. 2. In the figure,  $G_e$  and  $G_h$  stand for electron and hole thermionic emission rates and  $T_e$  and  $T_h$  denote electron and hole tunneling rates. Each carrier transition rate is formulated as follows,

$$G_e = v_{th} \sigma_n [n_i \exp\left(\frac{E_t - E_i}{kT}\right) - n_s (1 - f_t)] \quad (3)$$

$$G_h = v_{th} \sigma_p [n_i \exp\left(\frac{E_i - E_t}{kT}\right) - p_s f_t] \quad (4)$$

$$T_e = \frac{f_t - f_c}{\tau_e} \quad (5)$$

$$T_h = \frac{(1 - f_i) - (1 - f_v)}{\tau_h} \quad (6)$$

where  $\sigma_n$  and  $\sigma_p$  are electron and hole capture cross sections,  $\mathcal{E}_i$  and  $\mathcal{E}_t$  stand for the intrinsic Fermi-level and trap energy,  $f_v$ ,  $f_i$  and  $f_c$  are the electron occupation factors in the valence band, trap states and in the conduction band, respectively.  $n_s$  and  $p_s$  are electron and hole concentrations at the Si surface, which are calculated from a two-dimensional device simulation.  $\tau_e$  and  $\tau_h$  are electron and hole tunneling times from the WKB approximation. In a steady-state, the trap occupation factor  $f_i$  can be evaluated from the equality  $G_e + T_e = G_h + T_h$  with  $f_c \approx 0$  and  $f_v \approx 1$ . The three trap-assisted leakage current components are therefore expressed in the following [8],

$$\Delta I_{TAT} = qW \int_{\Delta L} \int_{bandgap} \Delta N_{it}(x, \mathcal{E}) \frac{T_e T_h}{G_e + T_e} d\mathcal{E} dx \quad (7)$$

$$\Delta I_{TF} = qW \int_{\Delta L} \int_{bandgap} \Delta N_{it}(x, \mathcal{E}) \frac{T_e G_h + T_h G_e}{G_e + T_e} d\mathcal{E} dx \quad (8)$$

$$\Delta I_{SRH} = qW \int_{\Delta L} \int_{bandgap} \Delta N_{it}(x, \mathcal{E}) \frac{G_e G_h}{G_e + T_e} d\mathcal{E} dx \quad (9)$$

where  $\Delta L$  is the width of the interface trap ( $\Delta N_{it}$ ) region and  $W$  is the channel width. The total trap-assisted leakage current  $\Delta I_d$  is the summation of the above three components,

$$\Delta I_d = \Delta I_{SRH} + \Delta I_{TF} + \Delta I_{TAT} \quad (10)$$

$$= qW \int_{\Delta L} \int_{bandgap} \Delta N_{it}(x, \mathcal{E}) (G_e + T_e) d\mathcal{E} dx$$

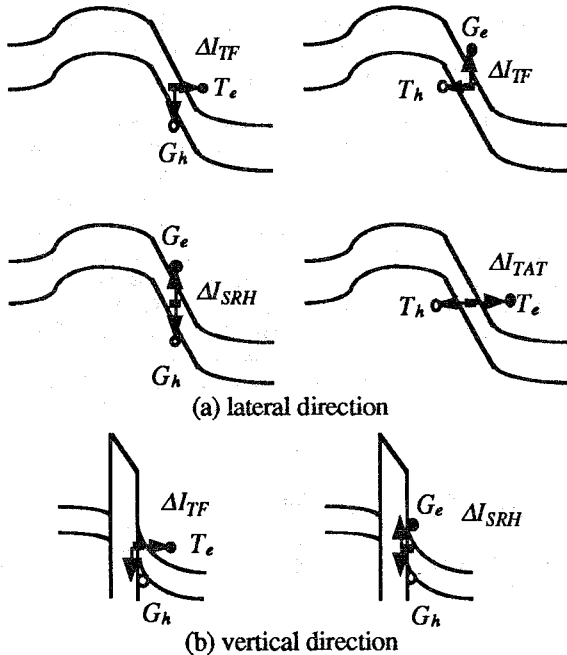


Fig. 2 Illustration of various carrier transition processes (a) in the

lateral direction and (b) in the vertical direction. Note that  $T_h$  only occurs in the lateral direction.

The temperature-dependent parameters used in the calculation are bandgap ( $\mathcal{E}_g$ ), thermal velocity ( $v_{th}$ ) and intrinsic concentration ( $n_i$ ). They are given below [11],

$$\mathcal{E}_g(T) = \mathcal{E}_g(0) - \alpha T^2 / (T + \beta) \quad (11)$$

$$v_{th} = \sqrt{3kT/m^*} \quad (12)$$

$$n_i = \sqrt{N_c N_v} \exp\left[-\frac{\mathcal{E}_g(T)}{2kT}\right] \quad (13)$$

The field-dependent parameters are  $\tau_e$  and  $\tau_h$ ,

$$\tau_e = \tau_{oc} \exp\left[\frac{4}{\hbar} (2m_n)^{1/2} (\mathcal{E}_c - \mathcal{E}_t)^{3/2}\right] \quad (14)$$

$$\tau_h = \tau_{ov} \exp\left[\frac{4}{\hbar} (2m_p)^{1/2} (\mathcal{E}_t - \mathcal{E}_v)^{3/2}\right] \quad (15)$$

where  $\tau_{oc}$  and  $\tau_{ov}$  are effective transit times in the conduction band and in the valence band,  $E_l$  is the surface field in the lateral direction and other variables have their usual definitions. Note that the hole tunneling  $T_h$  occurs only in the lateral direction. Thus,  $T_h$  is a function of only a lateral field whereas the tunneling process  $I_{BB}$  and  $T_e$  are dependent on a total field.

## DEVICE CHARACTERIZATION

The test device is a 0.35  $\mu\text{m}$  n-MOSFET with source/drain extension. The gate oxide thickness is about 40  $\text{\AA}$  and the gate width is 100  $\mu\text{m}$ . The device was subject to maximum substrate current stress  $V_{gs} = 2\text{V}$  and  $V_{ds} = 4.5\text{V}$  for 3000 seconds. The pre-stress and post-stress  $I_d - V_{gs}$  characteristics are shown in Fig. 3 ( $T = 292\text{K}$ ) and in Fig. 4 ( $T = 353\text{K}$ ), respectively. Under the stress condition, interface trap generation is almost saturated and oxide charge creation is minimal [7]. Interface trap generation is evidenced by the change of the subthreshold swing in Figs. 3 and 4. The DIBL effect is not significant in the device.

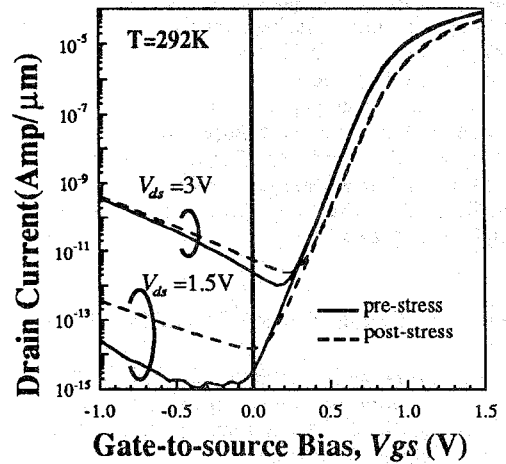


Fig. 3 Measured pre-stress and post-stress  $I_d - V_{gs}$  characteristics at  $V_{ds} = 1.5\text{V}$  and  $3.0\text{V}$ ,  $T = 292\text{K}$ .

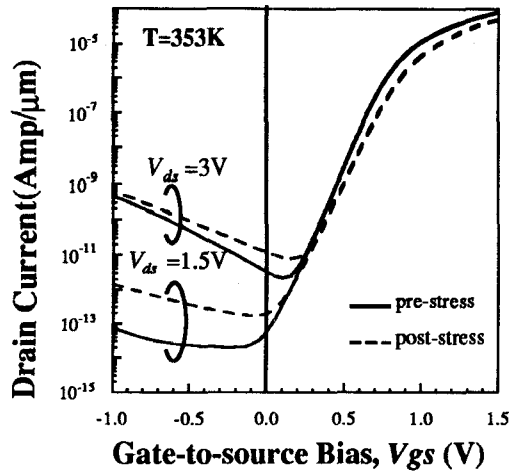


Fig. 4 Measured pre-stress and post-stress  $I_d$ - $V_{gs}$  characteristics at  $V_{ds}=1.5V$  and  $3.0V$ ,  $T=353K$ .

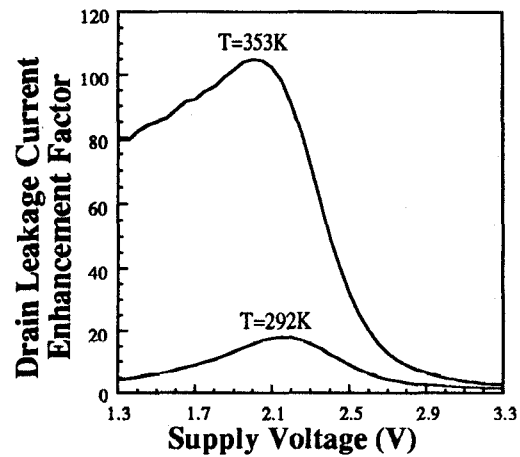


Fig. 6 The ratio of the post-stress drain leakage current to the pre-stress ( $T=292K$ ) drain leakage current versus supply voltage.

## RESULTS AND DISCUSSIONS

The dependence of pre-stress and post-stress drain leakage currents on supply voltage ( $V_{dd}$ ) is measured in Fig. 5. The leakage current enhancement factor, defined as the ratio of the post-stress drain leakage to the pre-stress drain leakage at  $T=292K$ , is shown in Fig. 6. The trap effect on the leakage current enhancement becomes particularly pronounced around a supply voltage of 2.2V. An enlargement of the drain leakage current by a factor of 18 is observed at  $T=292K$ . Various drain leakage current components  $I_{BB}$ ,  $I_S$  and the trap induced  $\Delta I_d$  are plotted in Fig. 7. The solid lines are the measured result and the circles represent the calculated result.

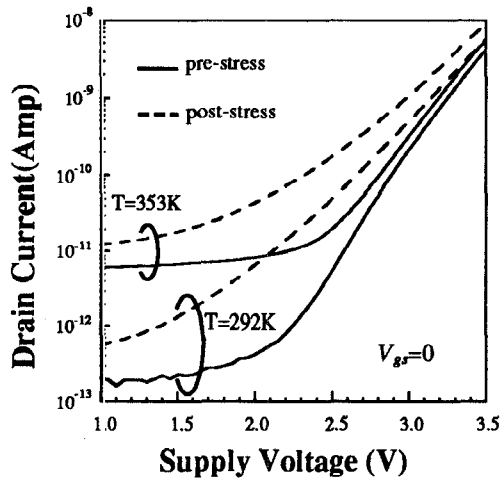


Fig. 5 Measured drain leakage current characteristics before and after stress at two different temperatures,  $T=292K$  and  $T=353K$ .

The interface trap density  $N_{it}$  used in the calculation is  $1.4 \times 10^{12} \text{cm}^{-2}$  and the length of the trap distribution ( $\Delta L$ ) is  $400 \text{\AA}$ .  $\sigma_n$  and  $\sigma_p$  in Eqs. (3) and (4) are  $10^{-15} \text{cm}^2$  [11]. The following features are observed. At a large supply voltage ( $V_{dd} \geq 3.0V$ ), the band-to-band tunneling current ( $I_{BB}$ ) manifests itself as a dominant mechanism even in a stressed device. In addition, the trap induced component  $\Delta I_d$  exhibits a weaker field dependence than the  $I_{BB}$  due to a smaller tunneling barrier from traps to the conduction band (electron tunneling) or to the valence band (hole tunneling). As a result, as the supply voltage scales, the  $I_{BB}$  drops more quickly and the  $\Delta I_d$  appears to be a major drain leakage mechanism in a stressed device. When the  $V_{dd}$  is further reduced, the tunneling effect becomes unimportant. The enhancement of the drain leakage is achieved mainly through the SRH component. Therefore, the enhancement factor in Fig. 6 peaks around 2.2V. At  $T=353K$ , the enhancement factor in Fig. 6 is significantly increased up to 110. The temperature effect is apparent at a lower  $V_{dd}$ . The enhancement factor at  $V_{dd}=1.3V$  increases from about 5 at  $T=292K$  to 80 at  $T=353K$ . The  $I_{BB}$ ,  $I_S$  and the  $\Delta I_d$  at  $T=353K$  are shown in Fig. 8.

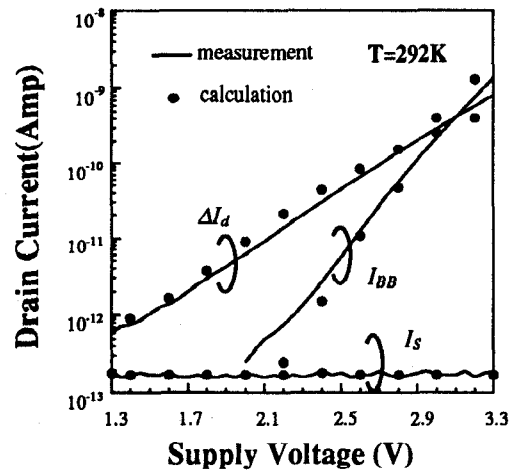


Fig. 7 Various drain leakage current components at  $T=292K$  from measurement (solid lines) and calculation (full circles).

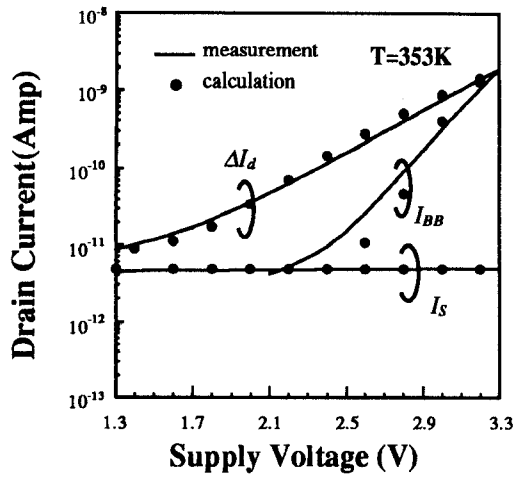


Fig. 8 Various drain leakage current components at T=353K from measurement (solid lines) and calculation (full circles).  $\Delta I_d$  represents the trap-induced drain leakage.

Furthermore, the components in the  $\Delta I_d$  are analyzed in Fig. 9 (T=292K) and in Fig. 10 (T=353K). In Fig. 9, the trap-induced drain leakage is dictated by the  $\Delta I_{TAT}$  for  $V_{dd} > 1.7V$ , by the  $\Delta I_{TF}$  for  $1.7V \geq V_{dd} \geq 1.5V$ , and by the  $\Delta I_{SRH}$  for  $1.5V \geq V_{dd}$ . In Fig. 10, the thermally related components  $\Delta I_{TF}$  and  $\Delta I_{SRH}$  are more prominent. As the supply voltage scales, the field dependent current component ( $\Delta I_{TAT}$ ) can be greatly alleviated, while the temperature dependent components ( $\Delta I_{TF}$  and  $\Delta I_{SRH}$ ) become dominant drain leakage mechanisms.

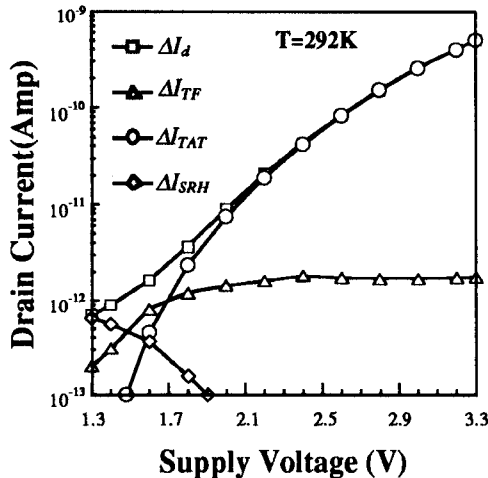


Fig. 9 Calculation of various interface trap induced drain leakage current components at T=292K.

The vertical field and the lateral field effects on drain leakage current are also assessed. Our calculation reveals that the band-to-band tunneling current is mainly contributed by the vertical field whereas the trap-assisted tunneling is mostly determined by the lateral field due to the dependence of  $T_h$  (hole tunneling) only on the lateral field.

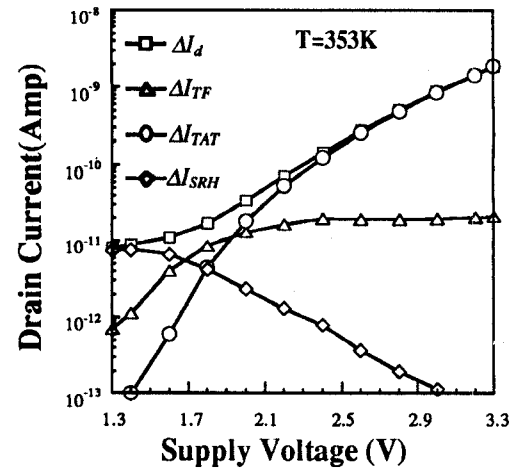


Fig. 10 Calculation of various interface trap induced drain leakage current components at T=353K.

## CONCLUSIONS

The band-to-band tunneling current is found to be a dominant drain leakage mechanism at  $V_{dd} = 3.3V$  in the current device structure. At a reduced supply voltage, the trap-induced current appears to be the major leakage component. We have observed that hot carrier stress can degrade the drain leakage current by orders of magnitude. While the vertical field has a larger effect on the band-to-band tunneling current, the trap-induced leakage is mostly caused by lateral field enhanced tunneling. The reduction of lateral field is necessary to suppress the trap-induced drain leakage in deep submicron devices.

## ACKNOWLEDGEMENT

Financial support from National Science Council, ROC, is gratefully acknowledged. The authors also would like to express thanks to Dr. Chimoon Hung at Macronix Inc. for many fruitful discussions.

## REFERENCES

- [1] J. Chen, T.Y. Chan, P.K. Ko, and C. Hu, 'Subbreakdown Drain Leakage Current in MOSFET,' *IEEE Electron Device Lett.* Vol. EDL-8, pp. 515-517, 1987.
- [2] T. Tsuchiya, "Trapped-electron and Generated Interface Traps in Hot Electron Induced MOSFET Degradation," *IEEE Trans. Elect. Dev.*, Vol. ED-34, pp. 2291-2296, 1987.
- [3] T. Wang, C. Huang, P. C. Chou, S. S. Chung and T. E. Chang, "Effects of Hot Carrier Induced Interface State Generation in Submicron LDD MOSFET's." *IEEE Trans. Elect. Dev.*, Vol. ED-41, pp. 1618-1622, 1994.
- [4] H. Sasaki, M. Saitoh, and K. Hashimoto, "Hot-carrier Induced Drain Leakage Current in n-channel MOSFET," in *IEDM Tech. Dig.*, pp. 726-729, 1987.
- [5] C. Duvvury, D. J. Redwine, and H. J. Stiegler, "Leakage Current Degradation in N-MOSFET's due to Hot-electron Stress," *IEEE Electron Device Lett.*, Vol. EDL-9, pp.579-581, 1988.
- [6] G. Q. Lo, A. B. Joshi, and D-L, Kwong, "Hot-carrier-stress Effects on Gate-induced Drain Leakage Current in n-channel MOSFET's." *IEEE Electron Device Lett.*, Vol. EDL-12, pp. 5-7, 1991.
- [7] A. Frommer, M. R. Pinto, and J. D. Bude, "Two-Stage Leakage Degradation in Sub-Micron MOSFET Technology", *Symp. on VLSI Tech.*, pp.164-165, 1996

- [8] T. Wang, T. E. Chang, and Chmoon Hung, "Interface Trap Induced Thermionic and Field Emission Current in Off-State MOSFET's" in *IEDM Tech. Dig.*, pp.161-164, 1994.
- [9] C. T. Wang, *Hot Carrier Design Consideration for MOS Devices and Circuits*, Van Nostran Reinheld, 1992
- [10] T. Y. Chan, J. Chen, P. K. Ko, and C. Hu, "The Impact of Gate-induced Drain Leakage Current on MOSFET Scaling," in *IEDM Tech. Dig.*, pp. 721-724, 1987.
- [11] S. M. Sze, *Semiconductor Device Physics and Technology* , John Wiley & Sons, 1985.